Nanoscale

COMMUNICATION

View Article Online
View Journal | View Issue

Cite this: *Nanoscale*, 2022, **14**, 6771

Received 17th December 2021,
Accepted 12th February 2022

DOI: 10.1039/d1nr08311b

rsc.li/nanoscale

Nanosegregation in arene-perfluoroarene π-systems for hybrid layered Dion–Jacobson perovskites†

Masaud Almalki,‡[a] Algirdas Dučinskas,‡[a,b] Loï C. Carbone,‡[a] Lukas Pfeifer,[a] Laura Piveteau,[c] Weifan Luo,[d] Ethan Lim,[d] Patricia A. Gaina,§[d] Pascal A. Schouwink,[e] Shaik M. Zakeeruddin,[a] Jovana V. Milić*[a,d] and Michael Grätzel*[a]

[a]*Laboratory of Photonics and Interfaces, Institute of Chemistry and Chemical Engineering, École Polytechnique Fédérale de Lausanne, 1015 Lausanne, Switzerland. E-mail: michael.graetzel@epfl.ch*
[b]*Max Planck Institute for Solid State Research, 70569 Stuttgart, Germany*
[c]*Institute of Chemistry and Chemical Engineering, École Polytechnique Fédérale de Lausanne, 1015 Lausanne, Switzerland*
[d]*Adolphe Merkle Institute, University of Fribourg, 1700 Fribourg, Switzerland. E-mail: jovana.milic@unifr.ch*
[e]*Institute of Chemistry and Chemical Engineering, École Polytechnique Fédérale de Lausanne, 1951 Sion, Switzerland*

†Electronic supplementary information (ESI) available. See DOI: 10.1039/d1nr08311b. Datasets presented here can be accessed at the DOI: 10.5281/zenodo.6194713 under the license CC-BY-4.0 (Creative Commons Attribution 4.0 International).

‡These authors contributed equally to the study.

§P. A. G. is presently affiliated with Alexandru Ioan Cuza University of Iasi, Faculty of Chemistry, Bd. Carol I, no. 11, 700506 Iasi, Romania.

Jovana V. Milić

Jovana V. Milić is Assistant Professor at the Adolphe Merkle Institute of the University of Fribourg in Switzerland. Her research focuses on the development of (supra)molecular materials for energy conversion, with a particular interest in photovoltaics. She has been recognized by the Periodic Table of Younger Chemists and as CAS Future Leader in 2019, Green Talent Award in 2020, and Zeno Karl Schindler Prize in 2021. She is invested in science outreach, policy and education, such as through activities of the European Young Chemists' Network and International Younger Chemists Network, connecting and supporting young scientists globally.

Layered hybrid perovskites are based on organic spacers separating hybrid perovskite slabs. We employ arene and perfluoroarene moieties based on 1,4-phenylenedimethylammonium (PDMA) and its perfluorinated analogue (F-PDMA) in the assembly of hybrid layered Dion–Jacobson perovskite phases. The resulting materials are investigated by X-ray diffraction, UV-vis absorption, photoluminescence, and solid-state NMR spectroscopy to demonstrate the formation of layered perovskite phases. Moreover, their behaviour was probed in humid environments to reveal nanoscale segregation of layered perovskite species based on PDMA and F-PDMA components, along with enhanced stabilities of perfluoroarene systems, which is relevant to their application.

Introduction

Layered hybrid perovskites (or 2D perovskites) are derived from three-dimensional organic–inorganic perovskites of general formula AMX_3 (Fig. 1a).[1–3] Here, A is the central cation (*e.g.* methylammonium MA^+, formamidinium FA^+, or Cs^+), M a divalent metal ion (mostly Pb^{2+} or Sn^{2+}) and X a halide anion (I^-,Br^-, or Cl^-).[4,5] The incorporation of a larger spacer cation between hybrid perovskite slabs can lead to the formation of 2D perovskite architectures, which have attracted attention due to their enhanced stabilities and versatility as compared to their 3D counterparts (Fig. 1b and c).[6–8] In particular, two classes of 2D perovskite materials are of special interest, namely the Ruddlesden–Popper (RP) and Dion–Jacobson (DJ) phases.[9–14] RP systems mostly follow the general formula $S'_2A_{n-1}M_nX_{3n+1}$, where S′ are monofunctional spacers that interact with the perovskite slabs by forming a bilayer with a half-a-unit-cell displacement between the perovskite slabs (Fig. 1b).[7,15] On the contrary, DJ systems are commonly based on the general formula $SA_{n-1}M_nX_{3n+1}$ incorporating bifunctional spacer (S) moieties between aligned perovskite slabs (Fig. 1c).[16] While RP phases have been widely used in perovs-

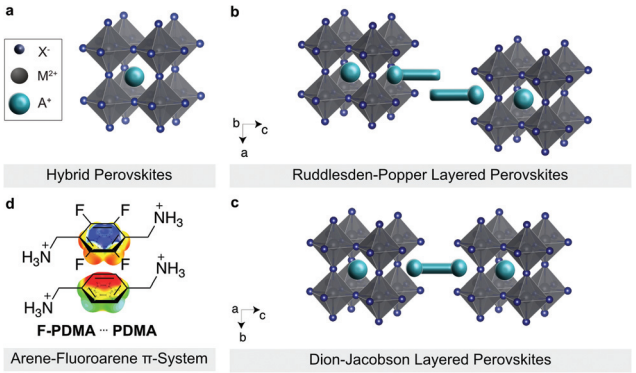

Fig. 1 Structural representation of (a) 3D and (b and c) 2D layered hybrid perovskite structures, highlighting (b) Ruddlesden–Popper and (c) Dion–Jacobson phases. The grey octahedra represent {PbX_6} frameworks whereas cyan rods illustrate the organic spacers. (d) Schematics of a π-stacking of arene and perfluoroarene moieties, namely 1,4-phenylenedimethylammonium (PDMA) and its analogue containing a perfluorinated phenylene moiety (F-PDMA).

kite optoelectronics, DJ phases are underrepresented despite their appealing optoelectronic properties and environmental stability.[17–20] It is thereby of interest to understand and control their structural and optoelectronic properties, which are highly dependent on the supramolecular self-assembly of the organic spacer layer.

A complementary pair of organic spacers could engage in π–π interactions, *e.g.* between arene and perfluoroarene species, through self-assembly to form an alternating-cation 2D perovskite system.[21] This has been previously analysed based on 2-phenylethylammonium (PEA) and 2-(perfluorophenyl)ethylammonium (FEA), forming an RP phase.[21] Such a favourable interaction is based on the complementarity between the quadrupole moments of the aromatic rings that is expected to yield a more compact parallel (π–π) stacking in arene-perfluoroarene systems (Fig. 1d).[21–26] This could alter the optoelectronic properties of the hybrid material.[14,16,27–29] In addition, the fluoroarene moieties are expected to increase hydrophobicity and reduce halide ion migration through π-ion interactions, which is relevant for the stability of the resulting materials.[24,26,30–32] Such tailored arene-perfluoroarene π-interactions, however, remain unexploited in controlling the properties of DJ perovskite phases.[16,21,26,33]

Here, we investigate a DJ system employing arene and perfluoroarene species, namely 1,4-phenylenedimethylammonium (PDMA) and its analogue comprising a perfluorinated phenylene moiety (F-PDMA), as well as their mixture (1 : 1 PDMA/F-PDMA, denoted as PF). We evidence the formation of layered perovskite structures by X-ray diffraction (XRD), accompanied by changes in the optoelectronic properties *via* UV-vis absorption and photoluminescence (PL) spectroscopy. We further demonstrate the formation of nonsegregated structures by solid-state NMR spectroscopy, while revealing enhanced environmental stability in humid environments, which is relevant to their future application.

Results and discussion

Thin films of layered perovskites were prepared based on $SPbI_4$ (n = 1) compositions (S = PDMA, F-PDMA (Fig. S1–S3†), and 1 : 1 PDMA : F-PDMA, denoted as PF) by solution-processing followed by annealing, in accordance with the procedure reported in the ESI.†

Structural properties were investigated by X-ray diffraction (XRD) in the Bragg–Brentano configuration (Fig. 2). The XRD patterns of the thin films show low angle reflections (<10°) at 2θ of 7.22°, 6.93° and 7.17° for (PDMA)PbI_4, (F-PDMA)PbI_4 and (PF)PbI_4, respectively, which is accompanied by periodic patterns typical of layered (2D) perovskite structures.[27,29,34,35] This is particularly the case for (PDMA)PbI_4 (Fig. 2a), whereas (F-PDMA)PbI_4 shows lower intensity peaks with a poor signal-to-noise ratio, suggesting lower crystallinity (Fig. 2b). We further observed a low angle diffraction for the mixed (PF)PbI_4 system characteristic for 2D structures, with an increase in relative intensity of the 14° and 28° diffraction peaks (Fig. 2c). This suggests that the presence of F-PDMA modifies out-of-plane texture of the films. To corroborate this, we analysed the films by grazing incidence wide angle X-ray scattering (GIWAXS) measurements (Fig. 2d–f and Fig. S4, ESI†). Films with different (5%, 10%, 25% and 50%) F-PDMA content were investigated (denoted as 5%, 10%, 25%, and 50% (PF), respect-

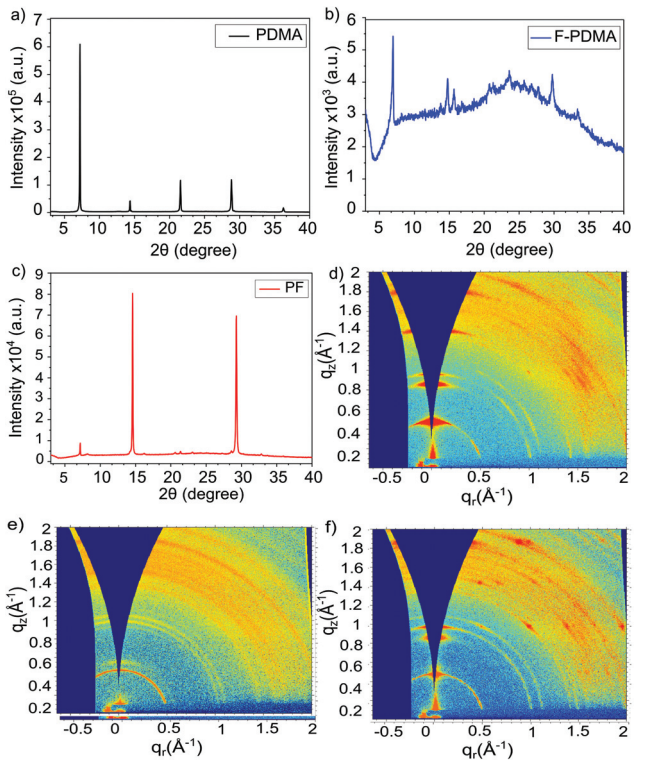

Fig. 2 Structural properties of layered hybrid perovskites. (a–c) XRD patterns of thin films based on (a) (PDMA)PbI_4 (black), (b) (F-PDMA)PbI_4 (blue), and (c) (PF)PbI_4 (red) compositions on microscope glass. (d–f) GIWAXS patterns of thin films of (d) (PDMA)PbI_4, (e) (F-PDMA)PbI_4, and (f) (PF)PbI_4. Methods and further analysis is provided in the ESI.†

ively) and compared to the PDMA-based 2D perovskite composition. We observe a very clear dependency of out-of-plane texture on F-PDMA content, which is confirmed by gamma integrations of the diffraction intensity at 7.3° (Fig. S5, ESI†). Likewise, a visual inspection of GIWAXS images shows that (PDMA)PbI_4 crystallites have a preferred orientation,[9–12,27,34] whereas upon the gradual addition of F-PDMA continuous Debye–Scherrer rings appear, indicating a more random distribution of crystallites (Fig. 2d–f and Fig. S4, ESI†). This suggests that F-PDMA inhibits the formation of texture in the films of PF-based compositions, which is likely a consequence of competing fluorine-based interactions in F-PDMA-based systems, in accordance with previous reports.[26,33]

The atomic-level interactions were further analysed by solid-state nuclear magnetic resonance (NMR) spectroscopy (Fig. 3).[34] Solid-state NMR has emerged as a powerful method to characterize the atomic-level structure of lead-halide perovskite materials.[36–42] To shed light on the coordination and distribution of the spacer ligands within the DJ phases, we relied on our previously developed approach.[21] Specifically, ^{19}F NMR spectra were recorded for the fluorinated spacer (F-PDMA) and a mechanosynthetic mixture of the two spacers (F-$PDMAI_2$ and $PDMAI_2$ stoichiometric 1 : 1 mixture, denoted as PF (Fig. 3a)), as well as their corresponding 2D perovskites, namely (F-PDMA)PbI_4 and (PF)PbI_4 (Fig. 3b). The ^{19}F NMR spectra of the F-PDMA spacer in pure state and within a mixture with PDMA were found to be identical, featuring two fluorine signals at −135 and −139 ppm, indicating that the chemical surrounding of the fluorine atoms is the same in both samples. This suggests that the $PDMAI_2$ and F-$PDMAI_2$ powders do not form a homogeneous phase upon mixing, but remain spacially separated within microcrystalline grains constituted of only one of the two molecules. However, the ^{19}F NMR spectra of 2D perovskites substantially change as compared to the spectrum of the pristine spacer, with different intensity ratios of the ^{19}F NMR signals, indicating the formation of new phases. This evidences that the fluorine atoms experience a different chemical surrounding within the perovskite material, in agreement with the incorporation of F-PDMA into the perovskite structure.

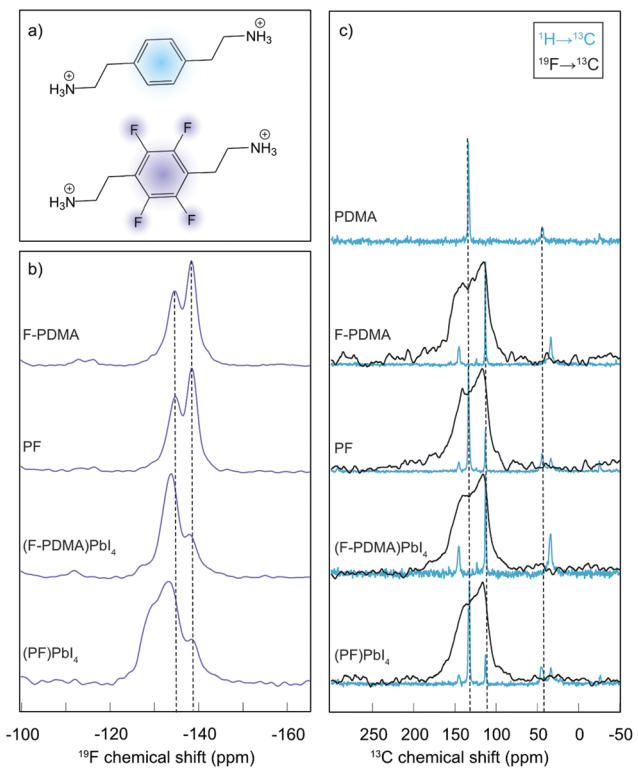

Fig. 3 Atomic-level structure of layered hybrid perovskites. (a) Structural representation of PDMA (top) and F-PDMA (bottom). (b) ^{19}F NMR spectra of F-$PDMAI_2$(F-PDMA), 1 : 1 spacer mixture (PF), and the corresponding 2D perovskites. (c) ^{13}C CP NMR spectra of arene spacer (PDMA), the perfluoroarene analogue (F-PDMA), a mixture of the two spacers (PF) as well as their 2D perovskite structures. The ^{13}C spectra obtained by transferring polarization from ^{1}H to ^{13}C are depicted in dark blue and the spectra obtained when transferring polarization from ^{19}F to ^{13}C are depicted in black.

Similarly, ^{19}F NMR of a 2D perovskite phase based on a 1 : 1 spacer mixtures (PF) reveals the formation of a different phase as it exibits an additional signal at *ca.* −130 ppm, whereas the other two signals remain almost unchanged in intensity and chemical shift. This is in accordance with nanosegregation into domains within the 2D perovskite material in which all spacers are fluorinated, forming the same phase as in materials prepared exclusively from F-PDMA. The additional signal at −130 ppm could either originate from the fluorinated spacers at the interface of these domains or from the domains where F-PDMA and PDMA form a homogeneous mixture. We have investigated this further by comparing ^{13}C cross-polarisation (CP) NMR spectra obtained by transferring polarisation either from ^{1}H or from ^{19}F nuclei (Fig. 3c and detailed in the ESI†). While the resolution of the $^{19}F \rightarrow {}^{13}C$ CP NMR spectra was insufficient to extract any additional structural insight, $^{1}H \rightarrow {}^{13}C$ CP NMR corroborates the co-existence of independent phases, each comprising only one spacer, in the mixed system, further evidencing their nanosegregation. In summary, solid-state NMR further confirms that F-PDMA is integrated into the DJ 2D perovskite structure, while evidencing that the mixture of spacers (F-PDMA and PDMA) leads to phase segregation, which is in accordance with a previous report on perfluorinated spacers in RP phases.[21] These structural changes are directly reflected in the optoelectronic properties of the films.

The optical properties of the thin films were analysed by UV-vis absorption and PL spectroscopy. The excitonic features in the absorption spectrum in the range of 490–500 nm are in agreement with the formation of layered 2D structures.[9,29,34] For (PDMA)PbI_4, (F-PDMA)PbI_4 and (PF)PbI_4, absorption maxima were observed at 510 nm, 480 nm, and 505 nm, respectively (Fig. 4a). Thin films containing mixtures of arene and perfluoroarene spacers with increasing amounts of F-PDMA (5%, 10%, and 25%) feature a gradual blue shift of the absorption maximum to 510 nm, 509 nm, and 507 nm, respectively (Fig. S5, ESI†). Similarly, PL spectra (Fig. 4b and

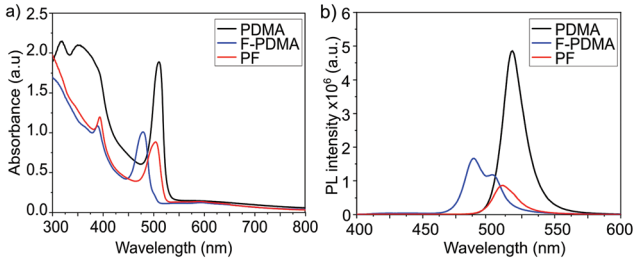

Fig. 4 Optoelectronic properties of layered hybrid perovskites. (a) UV-vis absorption spectra and (b) PL spectra of thin films based on (PDMA)PbI_4 (black), (F-PDMA)PbI_4(blue), and (PF)PbI_4 (red) on microscope glass. Further characteristics are shown in the ESI.†

Fig. S5, ESI†) show minor Stokes shifts of *ca.* 20 nm, 10 nm, and 15 nm for (PDMA)PbI_4, (F-PDMA)PbI_4 and (PF)PbI_4, respectively, accompanied by a gradual reduction in photoluminescence quantum yield (PLQY) related to their excitonic characteristics (Fig. S6, ESI†), confirming that the presence of F-PDMA has an impact on the optical properties. The corresponding PL spectra of neat F-PDMA-based thin films also appear to involve multiple signals, which is likely associated with their structural disorder and requires further investigation.

Having evidenced the 2D perovskite formation through optical and structural properties, the stability of the materials was analysed by monitoring the behaviour of the films in humid environments.[34,43] For this purpose, we measured contact angles (Fig. S7, ESI†) for the films based on F-PDMA, PDMA and with various amounts of F-PDMA (5%, 10%, 25% and 50% (PF)) with respect to PDMA in 2D perovskite compositions. With increasing F-PDMA content from 0%, over 5%, 10%, 25%, up to 50%, contact angles of 49.6°, 59.6°, 62.1°, 63.3°, and 60.1° were obtained, respectively, showing a substantial increase in hydrophobicity in the presence of F-PDMA. The system based on 25% F-PDMA demonstrated the greatest hydrophobicity, which was accompanied by the highest intensity of diffraction peaks that are commonly associated with the crystallites of perovskite layers that are perpendicular to the substrate (Fig. S5, ESI†).[34] This suggests that the changes in hydrophobicity are likely not only associated with the fluoroarene content but also with the orientation of crystallites and the organic spacers in the films. The environmental stability was further assessed by measuring optical (UV-vis absorption and PL spectra) as well as structural properties (XRD) after exposing the samples to a relative humidity of 80 ± 5% for 15 min. While (PDMA)PbI_4 is known to hydrate in humid conditions (Fig. 5a),[9,34,44] (F-PDMA)PbI_4 did not undergo any change (Fig. 5b). However, the UV-vis absorption spectra of mixed (PF)PbI_4 films changed when exposed to humid conditions (Fig. 5c), with a 25 nm blue shift of the absorption peak at 510 nm and an increase of absorbance in the 405 nm region. Furthermore, recorded XRD patterns (Fig. 5d) reveal a transformation that could be depicted as a superimposition of the patterns of two species, *i.e.* the hydrated PDMA-based phase and the co-existing (F-PDMA)PbI_4 phase.

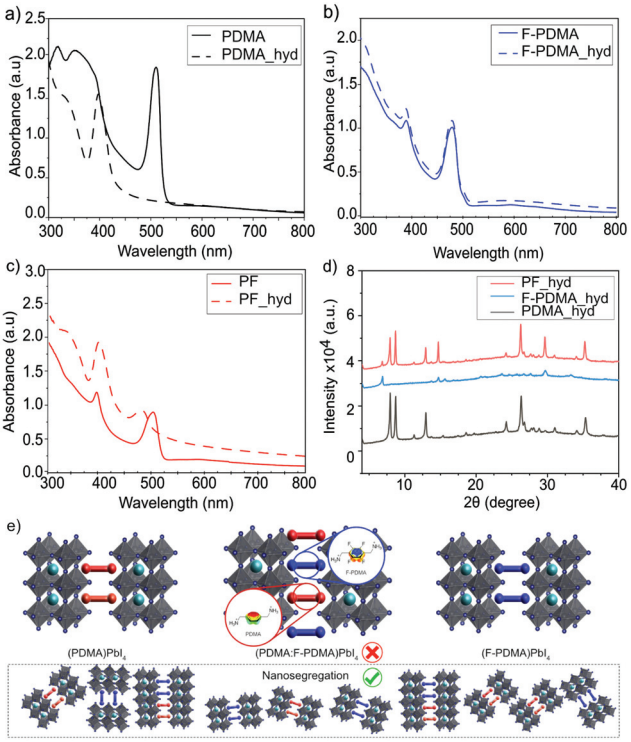

Fig. 5 Environmental stability of layered hybrid perovskites. (a–c) UV-vis spectra of (PDMA)PbI_4 (black), (F-PDMA)PbI_4 (blue), and (PF)PbI_4 (red) on microscope glass before (plain lines) and after (dashed lines) exposure to a relative humidity of 80 ± 5% for 15 min. (d) XRD patterns of (PDMA)PbI_4 (black), (F-PDMA)PbI_4 (blue), and (PF)PbI_4 (red) on microscope glass after exposure to humid conditions (referred to as hyd). (e) Schematic representation of layered and nanosegregated PDMA/F-PDMA perovskite structures.

This observation is in accordance with the formation of a segregated structure of the perovskite phases based on two spacer moieties in mixed thin films (Fig. 5e), as indicated by solid-state NMR spectroscopy. Since PDMAI-based films are known to hydrate, whereas F-PDMAI-based ones are resistant to hydration, the mixed cation system is expected to be more resilient to moisture. Instead, the formation of a hydrated PDMA phase suggests that, in contrast to the previous reports on arene-fluoroarene-based systems,[30,45] the corresponding DJ systems remain nanosegregated. This process has been previously associated with improvements in photovoltaic performances and operational stabilities,[21] which is relevant for the application of these materials in the future.

Conclusions

In summary, we investigated arene and perfluoroarene spacers, namely 1,4-phenylenedimethylammonium (PDMA) and its analogue containing a perfluorinated moiety (F-PDMA), for their propensity to form hybrid Dion–Jacobson layered perovskite materials through self-assembly. The analysis showed that PDMAI, F-PDMA, and their 1 : 1 mixture form

layered perovskite materials, which are not well oriented in the case of F-PDMA-based films. Moreover, while the F-PDMA-based system showed resilience to moisture, its addition to the PDMA-based composition did not prevent hydration, suggesting the possible formation of a segregated structure which was confirmed by solid-state NMR spectroscopy. This provides insights for the design of Dion–Jacobson perovskites incorporating arene-perfluoroarene π-systems, stimulating further studies towards their application in optoelectronics.

Data availability

All data presented here can be accessed at DOI: 10.5281/zenodo.6194713 and it is available under the license CC-BY-4.0 (Creative Commons Attribution 4.0 International).

Author contributions

The manuscript was written by M.A., J.V.M., A.D., L.P., and L.C.C. through support of all the co-authors. The study was conceptualized by J.V.M. who supervised L.C.C., M.A., E.L., W.L. and P.A.G. throughout the project. L.C.C. synthesized the organic spacer materials under the supervision of L.P., and he fabricated and characterized thin-films with the support of A.D., who also performed the mechanosynthesis of powders. W.L., E.L., and P.A.G. synthesized and characterized the organic spacer materials and the corresponding thin-films as well as mechanosynthesized powders to complement the investigation of their structural and optoelectronic properties, in particular by solid-state NMR spectroscopy, which was performed by L.Pi. S.M.Z. was involved in the discussions and the supervision of L.C.C. and M.A., while M.G. directed the project. All authors contributed to the writing process and approved the final version of the manuscript.

Conflicts of interest

There are no conflicts to declare.

Acknowledgements

A. D. and M. G. are grateful to the Max Planck Society and its EPFL Center for financial support. J. V. M. acknowledges SNSF PRIMA grant no. 193174. E. L. and J. V. M. are grateful to the NCCR Bioinspired Materials program for support in the course of the study. M. A. gratefully acknowledges KACST for the fellowship. We would like to thank Dr Felix Eickemeyer (Laboratory of Photonics and Interfaces, EPFL) for support with the PLQY measurements and Dr Yum Jun Ho (Laboratory of Molecular Engineering of Optoelectronic Nanomaterials, EPFL) for help with contact angle measurements.

References

1 A. Poglitsch and D. Weber, *J. Chem. Phys.*, 1987, **87**, 6373–6378.
2 O. Knop, R. E. Wasylishen, M. A. White, T. S. Cameron and M. J. V. Oort, *Can. J. Chem.*, 1990, **68**, 412–422.
3 A. Kojima, K. Teshima, Y. Shirai and T. Miyasaka, *J. Am. Chem. Soc.*, 2009, **131**, 6050–6051.
4 N. Pellet, P. Gao, G. Gregori, T.-Y. Yang, M. K. Nazeeruddin, J. Maier and M. Grätzel, *Angew. Chem.*, 2014, **126**, 3215–3221.
5 A. K. Jena, A. Kulkarni and T. Miyasaka, *Chem. Rev.*, 2019, **119**, 3036–3103.
6 I. C. Smith, E. T. Hoke, D. Solis-Ibarra, M. D. McGehee and H. I. Karunadasa, *Angew. Chem., Int. Ed.*, 2014, **53**, 11232–11235.
7 G. Grancini and M. K. Nazeeruddin, *Nat. Rev. Mater.*, 2019, **4**, 4–22.
8 H. Ren, S. Yu, L. Chao, Y. Xia, Y. Sun, S. Zuo, F. Li, T. Niu, Y. Yang, H. Ju, B. Li, H. Du, X. Gao, J. Zhang, J. Wang, L. Zhang, Y. Chen and W. Huang, *Nat. Photonics*, 2020, **14**, 154–163.
9 Y. Li, J. V. Milić, A. Ummadisingu, J.-Y. Seo, J.-H. Im, H.-S. Kim, Y. Liu, M. I. Dar, S. M. Zakeeruddin, P. Wang, A. Hagfeldt and M. Grätzel, *Nano Lett.*, 2018, **19**, 150–157.
10 N. Parikh, M. M. Tavakoli, M. Pandey, A. Kalam, D. Prochowicz and P. Yadav, *Sustainable Energy Fuels*, 2021, **5**, 1255–1279.
11 S. Kahmann, H. Duim, A. J. Rommens, E. K. Tekelenburg, S. Shao and M. A. Loi, *Adv. Opt. Mater.*, 2021, 2100892.
12 G. Wu, R. Liang, Z. Zhang, M. Ge, G. Xing and G. Sun, *Small*, 2021, 2103514.
13 J. V. Milić, *J. Mater. Chem. C*, 2021, **9**, 11428–11443.
14 J. V. Milić, S. M. Zakeeruddin and M. Grätzel, *Acc. Chem. Res.*, 2021, **54**, 2729–2740.
15 H. Tsai, W. Nie, J.-C. Blancon, C. C. Stoumpos, R. Asadpour, B. Harutyunyan, A. J. Neukirch, R. Verduzco, J. J. Crochet, S. Tretiak, L. Pedesseau, J. Even, M. A. Alam, G. Gupta, J. Lou, P. M. Ajayan, M. J. Bedzyk, M. G. Kanatzidis and A. D. Mohite, *Nature*, 2016, **536**, 312–316.
16 L. Mao, W. Ke, L. Pedesseau, Y. Wu, C. Katan, J. Even, M. R. Wasielewski, C. C. Stoumpos and M. G. Kanatzidis, *J. Am. Chem. Soc.*, 2018, **140**, 3775–3783.
17 S. Ahmad, P. Fu, S. Yu, Q. Yang, X. Liu, X. Wang, X. Wang, X. Guo and C. Li, *Joule*, 2019, **3**, 794–806.
18 P. Huang, S. Kazim, M. Wang and S. Ahmad, *ACS Energy Lett.*, 2019, **4**, 2960–2974.
19 D. Lu, G. Lv, Z. Xu, Y. Dong, X. Ji and Y. Liu, *J. Am. Chem. Soc.*, 2020, **142**, 11114–11122.
20 Z. Xu, D. Lu, X. Dong, M. Chen, Q. Fu and Y. Liu, *Adv. Mater.*, 2021, 2105083.
21 M. A. Hope, T. Nakamura, P. Ahlawat, A. Mishra, M. Cordova, F. Jahanbakhshi, M. Mladenović, R. Runjhun, L. Merten, A. Hinderhofer, B. I. Carlsen, D. J. Kubicki, R. Gershoni-Poranne, T. Schneeberger, L. C. Carbone,

Y. Liu, S. M. Zakeeruddin, M. Grätzel, J. V. Milić and L. Emsley, *J. Am. Chem. Soc.*, 2021, **143**, 1529–1538.
22 C. Sutton, C. Risko and J.-L. Bredas, *Chem. Mater.*, 2016, **28**, 3–16.
23 K. S. Kim, P. Tarakeshwar and J. Y. Lee, *Chem. Rev.*, 2000, **100**, 4145–4186.
24 M. Giese, M. Albrecht and K. Rissanen, *Chem. Rev.*, 2015, **115**, 8867–8895.
25 D.-X. Wang and M.-X. Wang, *Acc. Chem. Res.*, 2020, **53**, 1364–1380.
26 Y. Liu, S. Akin, L. Pan, R. Uchida, N. Arora, J. V. Milić, A. Hinderhofer, F. Schreiber, A. R. Uhl, S. M. Zakeeruddin, A. Hagfeldt, M. I. Dar and M. Grätzel, *Sci. Adv.*, 2019, **5**, eaaw2543.
27 M. C. Gélvez-Rueda, P. Ahlawat, L. Merten, F. Jahanbakhshi, M. Mladenović, A. Hinderhofer, M. I. Dar, Y. Li, A. Dučinskas, B. Carlsen, W. Tress, A. Ummadisingu, S. M. Zakeeruddin, F. Schreiber, A. Hagfeldt, U. Rothlisberger, F. C. Grozema, J. V. Milić and M. Grätzel, *Adv. Funct. Mater.*, 2020, **30**, 2003428.
28 H. Fu, *J. Mater. Chem. C*, 2021, **9**, 6378–6394.
29 J.-C. Blancon, J. Even, C. C. Stoumpos, M. G. Kanatzidis and A. D. Mohite, *Nat. Nanotechnol.*, 2020, **15**, 969–985.
30 Z. Xu and D. Mitzi, *Chem. Mater.*, 2003, **15**, 3632–3637.
31 Y. Zhuang, P. Ma, J. Shi, H. Lin, G. You, G. Xu and B. Cai, *Adv. Mater. Interfaces*, 2021, 2101343.
32 M. A. Ruiz-Preciado, D. J. Kubicki, A. Hofstetter, L. McGovern, M. H. Futscher, A. Ummadisingu, R. Gershoni-Poranne, S. M. Zakeeruddin, B. Ehrler, L. Emsley, J. V. Milić and M. Grätzel, *J. Am. Chem. Soc.*, 2020, **142**, 1645–1654.
33 D. Wang, S.-C. Chen and Q. Zheng, *J. Mater. Chem. A*, 2021, **9**, 11778–11786.
34 A. Dučinskas, G. Y. Kim, D. Moia, A. Senocrate, Y.-R. Wang, M. A. Hope, A. Mishra, D. J. Kubicki, M. Siczek, W. Bury, T. Schneeberger, L. Emsley, J. V. Milić, J. Maier and M. Grätzel, *ACS Energy Lett.*, 2021, **6**, 337–344.
35 B. Saparov and D. B. Mitzi, *Chem. Rev.*, 2016, **116**, 4558–4596.
36 W. M. Franssen and A. P. Kentgens, *Solid State Nucl. Magn. Reson.*, 2019, **100**, 36–44.
37 G. M. Bernard, R. E. Wasylishen, C. I. Ratcliffe, V. Terskikh, Q. Wu, J. M. Buriak and T. Hauger, *J. Phys. Chem. A*, 2018, **122**, 1560–1573.
38 A. Senocrate and J. Maier, *J. Am. Chem. Soc.*, 2019, **141**, 8382–8396.
39 D. J. Kubicki, S. D. Stranks, C. P. Grey and L. Emsley, *Nat. Rev. Chem.*, 2021, **5**, 624–645.
40 C. J. Dahlman, D. J. Kubicki and G. M. Reddy, *J. Mater. Chem. A*, 2021, **9**, 19206–19244.
41 S. R. Smock, Y. Chen, A. J. Rossini and R. L. Brutchey, *Acc. Chem. Res.*, 2021, **54**, 707–718.
42 I. L. Moudrakovski, *Annu. Rep. NMR Spectrosc.*, 2021, **102**, 269.
43 U.-G. Jong, C.-J. Yu, G.-C. Ri, A. P. McMahon, N. M. Harrison, P. R. Barnes and A. Walsh, *J. Mater. Chem. A*, 2018, **6**, 1067–1074.
44 A. Dučinskas, G. C. Fish, M. A. Hope, L. Merten, D. Moia, A. Hinderhofer, L. C. Carbone, J.-E. Moser, F. Schreiber, J. Maier, J. V. Milić and M. Grätzel, *J. Phys. Chem. Lett.*, 2021, **12**, 10325–10332.
45 D. B. Mitzi, D. R. Medeiros and P. R. Malenfant, *Inorg. Chem.*, 2002, **41**, 2134–2145.